Transport of a Heavy Ion Beam in a Fusion Reactor Chamber With a Low Pressure Gas

S. Sudo

O/45 Sept.1980

MAX-PLANCK-INSTITUT FÜR PLASMAPHYSIK

8046 GARCHING BEI MÜNCHEN

MAX-PLANCK-INSTITUT FÜR PLASMAPHYSIK

GARCHING BEI MÜNCHEN

Transport of a Heavy Ion Beam in a Fusion Reactor Chamber With a Low Pressure Gas

S. Sudo

O/45 Sept.1980

Diese Arbeit wurde gefördert durch das
Bundesministerium für Forschung und Technologie

O/45 S. Sudo

Transport of a Heavy Ion Beam in a Fusion Reactor Chamber with a low Pressure Gas

Abstract

The final transport process of an intense ion beam for heavy ion fusion is considered. The condition dealt mainly is that the reactor chamber is filled with a rarefied lead gas ($\sim 10^{-5}$ torr). In spite of the low pressure of the background gas, the gas has much influence on focusing the beam through two effects, namely, stripping of the beam ions by the background gas and charge neutralization of the beam by the electrons produced from the gas. In the case of a rarefied lead gas, the repulsive force due to the high charge state is the dominant effect while it is contrary in the case of a rather high pressure nitrogen gas ($\sim$ 1 torr). Nevertheless, a focal radius can be within 3 mm under conditions of the entrance radius of 20 cm, the current of 1 kA, the emittance of 4×10^{-5} and the distance of 10 m from the entrance port of the chamber to the position of the target. The accuracy of the beam divergence at the entrance port should be within 0.5% if the variation of the spot radius at z = 10 m has to be limited within 10%.

I. Introduction

The final focusing of an ion beam in a pellet fusion reactor is considered. Up to now, there seem to be two interesting regimes for the conditions in the reactor chamber. One possibility is a rather high gas pressure ~ 1 torr [1,2]. In this region, the beam ions in the beam are rapidly stripped to a very high charge state by a background gas. The heavy ions with a high charge state effectively ionize the background gas so that the density of the electrons produced is much higher than that of the beam. Charge neutralization of the ion beam then easily occurs. This may be favorable to focusing the beam because repulsive forces due to space charge do not play a significant role any more. Otherwise, the space charge effect may be critical to focusing the beam under certain conditions. However, complicated phenomena such as multiple scattering by the background gas, knock-on electrons and self pinch force due to magnetic dissipation of the neutralizing current may also occur, although the two-stream instability will be damped by collisions if the density of the plasma produced is sufficiently high. The differential pumping at the interface (at the chamber wall or window) may be not easy because an accelerator should be highly evacuated.

Another possibility is in a liquid lithium lead ($Pb_{83}Li_{17}$) wall protection scheme [3]. In a typical case, the pressure of the background gas (lead) is 10^{-5} torr. This is much lower than that of the former case. However, the pumping is not very easy in this case either because the pressure at the time soon after the pellet burning may be much higher.

This paper mainly deals with focusing under the latter condition (10^{-5} torr lead gas). The neutralization effect due to ionized electrons from a gas in a reactor chamber is included. The emittance and space charge effects are adverse to focusing. The stripping of the heavy ion by a background gas is also bad for focusing because of the stronger electrostatic force due to a higher charge state, while a higher charge state is more effective in ionizing a background gas and the electrons produced neutralize the heavy ion beam.

The typical case to be considered consists of a beam of U^+ ions of 10 GeV with a current of 1 kA and a pulse length of 10 ns (the pulse length is no critical parameter in this study and the results can be applied in the case of a longer pulse just as well).

In this paper the pellet radius is assumed to be about 3 mm.

II. The Calculation Model

It is assumed that the beam is cylindrical in form and the particle distribution in the beam is homogeneous.

The outermost radius R of the ion beam can be determined by an envelope equation (e.g. Ref.[4]):

$$\frac{\partial^2 R}{\partial z^2} - \frac{g}{R} - \frac{\varepsilon^2}{R^3} = 0 \,, \qquad (1)$$

where $g = \dfrac{I Z_{eff}(1-f)}{2\pi\varepsilon_o m_o c^3 \beta^3 r^3}$ and ε is the emittance $(= R_o \cdot V_{th}/\beta c)$.

The following parameters are defined as:

Z_{eff} = effective charge of ion beam
I = current of ion beam (A)
f = charge neutralization ratio
m_o = mass of ion particle
β = ratio of the particle velocity to velocity of light
γ = $1/\sqrt{1-\beta^2}$
z = coordinate in the direction of beam propagation

The process of stripping of the uranium ion by the background gas is calculated using the cross sections given in Ref.[5].

The equations to get effective Z_{eff} are as follows:

$$\lambda_I = \frac{1}{n_g \sigma_I} \,, \qquad (2)$$

$$Z(z+\Delta z,1) = Z(z,1)\cdot(1-\Delta z/\lambda_1)$$
$$Z(z+\Delta z,I) = Z(z,I)\cdot(1-\Delta z/\lambda_I)+Z(z,I-1)\cdot\Delta z/\lambda_{I-1} \quad (2\leq I\leq 91) \qquad (3)$$
$$Z(z+\Delta z,92) = Z(z,92)+Z(z,91)\cdot\Delta z/\lambda_{91} \ ,$$
$$Z_{eff}(z) = \sum_{I=1}^{92} I\cdot Z(z,I) \ , \qquad (4)$$

where $Z(z,I)$ is the distribution function of the charge state I at the position z and n_g is the density of the background gas and σ_I is the stripping cross section of the charge state I of the uranium. The cross sections for lead are not given in Ref.[5]. In this case, the cross section of each level of the uranium ion is estimated by the classical binary collision model as follows:

$$\sigma_I = \frac{e^4}{8\pi\varepsilon_o^2 m_e c^2}\cdot\frac{Z_g^2}{\beta^2\Delta E_I} \ , \qquad (5)$$

where Z_g is the atomic number of the background gas and ΔE_I is the ionization potential of the uranium ion [6,7].

The electrons are produced through ionization of the background gas by the ion beam as follows:

$$\frac{\partial n_e}{\partial t} = \frac{I/e}{\pi R^2}\cdot\frac{S}{W} \ , \qquad (6)$$

where

n_e = the electron density
S = stopping power (Bethe formula)
W = the energy necessary for the production of an ion pair from the background gas atom (36 eV for H_2, 35 eV for N_2 in Ref.[8]).

In the present case of the background gas from $Pb_{83}Li_{17}$ alloy, the gas pressure of lead is 10^{-5} torr if the temperature of the liquid $Pb_{83}Li_{17}$ at the outlet of the chamber wall is 500° C. Under such a condition, the number of electrons produced is comparable with that of the ion particles in the beam and the space

charge is partially neutralized. Under such a condition, the electrons produced are trapped (in spite of the relative velocity βc to the heavy ions) by the large electrostatic potential of the ion beam during beam propagation in the chamber, while the ions produced remain at rest.

The numerically calculated equipotential curves are shown in Fig.1 for a beam radius of 10 cm. The potential difference between the potential at the edge of the cylinder axis and that at the center of the axis of the ion beam can be determined analytically as follows:

$$\Delta U = 7.53 \times 10^2 I/\beta R^2 \times (1-f) \times \left\{\frac{1}{4}\ell^2 + \frac{1}{2}\ell\left(\sqrt{R^2+\frac{1}{4}\ell^2} - \sqrt{R^2+\ell^2}\right) + \frac{R^2}{2}\ln\left(\frac{\frac{1}{2}\ell+\sqrt{R^2+\frac{1}{4}\ell^2}}{-\frac{1}{2}\ell+\sqrt{R^2+\frac{1}{4}\ell^2}} \cdot \frac{\sqrt{R^2+\ell^2}-\ell}{R}\right)\right\} \text{ (eV)} , \qquad (7)$$

where ℓ is the length of the beam. If ℓ = 1 m, β = 0.3, I = 1 kA, f = 0 and R = 0.1 m, then Δ U = 2.66 MeV.

After the trapped electrons are accumulated in the ion beam, the potential of the ion beam decreases until it equals the kinetic energy of the electrons with the velocity βc. If β = 0.3, the limiting potential for trapping is 24.7 keV. When the potential difference in the ion beam reaches this value, the electrons produced will not be trapped any more. This model is only applied if the density of the electrons produced within the pulse duration is less than that of the beam. If ΔU is considerably larger than 24.7 keV, the distribution of the relative velocities of the trapped electrons is sufficiently broad to suppress the two stream instability with gas ions. The emittance ε of the ion beam is assumed to be 4×10^{-5} rad·m. The distance from the entrance port to the target is fixed at 10 m. U^+ ions have an energy of 10 GeV ($\beta \sim 0.3$). The set of equations (1) to (6) with the potential condition described above is numerically resolved.

III. Results

The initial radius of the beam at the window of the chamber wall is taken as 20 cm. The pressure of the lead is assumed to be 10^{-5} torr and the partial pressure of the lithium can be neglected in our case.

At first, the change of the envelope radius in vacuum is shown in Fig.2a. The ion beam has a current of 1 kA. The beam divergence at the window is $\theta \equiv dR/dz\big|_{z=0} = -2.05 \times 10^{-2}$. The focal point is then at z = 10 m and the focal spot radius 2.20 mm, as shown in Fig.2a.

When the pressure of the lead gas is 10^{-5} torr, the focal spot radius becomes 3.0 mm and the focal point is 50 cm away from z = 10 m, as shown in Fig.2b. The spot size at z = 10 m is then 7.70 mm.

However, the value of θ can be adjusted to -2.13×10^{-2}, so that the focal point may again be at z = 10 m, as shown in Fig.3a. The focal spot radius at z = 10 m is now 2.81 mm (28% larger than that in vacuum case). It may be interesting to see how the spot size at z = 10 m is varied if the current is somewhat changed: with a current of 800 A, the spot radius at z = 10 m is 3.31 mm as shown in Fig.3b. The change from the case of 1 kA is 18% and the difference of the spot area is 39%. These values can be improved if the current only changes from 800 A to 1 kA. If we choose $\theta = -2.12 \times 10^{-2}$, we can then improve the above large difference, as shown in Fig.4a, b and c. In this case the spot sizes differ by 9% and the spot areas differ by 19%. It is possible to keep the change of the spot size constant within 10% in the current range 800 A ~ 1 kA only if θ can be adjusted with an accuracy of 0.5%.

In order to clarify the dependence of the spot size on the beam divergence θ, the curves of the spot size R_s at the position z = 10 m, the focal spot radius R_f and the deviation Δz of the focal point from z = 10 m varied with θ are shown in Fig.5. The values of I = 1 kA and p = 10^{-5} torr (lead) are fixed. The symbol

$\Delta\theta$ means $(-2.13 \times 10^{-2} - \theta)/2.13 \times 10^{-2}$. It is normalized to the case in Fig.3a. As shown in Fig.5, R_f has a weak dependence on $\Delta\theta$ while R_s is changed strongly with $\Delta\theta$. In practice, the position of the pellet is fixed. R_s is then more important than R_f for real focusing. If the maximum change of R_s has to be within 10%, the accuracy of θ should be within 0.5%. It is the same value in the previously discussed case of the change of the current.

A temporal change of the gas density may also be significant to focusing if θ is kept fixed. In fact, the spot size at z = 10 m under twice the pressure of Fig.4a is 4.03 mm, as shown in Fig.6a, which, of course, may not be tolerable. The dependence of R_s, R_f and Δz on the gas pressure p is shown in Fig.6b. R_s varies strongly with p. If the pressure is 10^{-4} torr, R_s is larger than 10 mm. However, θ can be adjusted to focus the beam to a reasonable radius at z = 10 m if the gas density is monitored and is coupled to the magnetic lens. This is clear because the value of R_f is even about 2 mm where p is more than 2×10^{-5} torr as shown in Fig.6b.

It may be interesting to compare the results with the case of a gas-filled (e.g. 1 torr nitrogen) reactor. The changes of the envelope radius, $Z_{eff}(z)$ and plasma-to-beam density ratio η with the distance from the entrance port are shown in Fig.7a. The value of θ is -2.00×10^{-2}. Z_{eff} and η are calculated with the two different models described in II. As shown in this figure, the discrepancy of the two curves is not large. R is calculated using the results with the classical binary collision model for comparison with the case of a rarefied lead gas. It is remarkable that the focal spot radius at z = 10 m is 2.00 mm, which is less than that of the vacuum case, as shown in Fig.2a, while the situation in the case of a rarefied lead gas is the contrary. The sufficient density of the electrons produced completely neutralizes the beam and is favorable to focusing. The instabilities, multiple scattering and self pinch effect are not included, which may be significant. The distributions of the charge state of the uranium ions at four different distances from the entrance port are also shown in Fig.7b.

The uranium ions are already highly stripped at z = 3 m. And even at a very early stage the density of the plasma produced is already much higher than that of the ion beam, whereas in the case of a rarefied lead gas the density of the plasma produced during the pulse duration (~ 10 ns) is much less than that of the ion beam and then the ion beam is only partially neutralized.

In case of a lead gas the cross sections calculated by the classical binary collision model might be more different from the real values than in the case of a nitrogen gas because the lead atoms have more electrons and more complicated effects (shielding effect etc.) might have to be included. Such data should be examined and confirmed by experiments. The changes of the values of R_s, R_f and Δz with the change of cross sections are shown in Fig.8. The cross sections are normalized to the value resulting from the classical binary collision model. The pressure of a lead gas ($p = 10^{-5}$ torr), the current ($I = 1$ kA) and $\theta = -2.12 \times 10^{-2}$ are fixed. The values of R_s and R_f are not so strongly changed in the region from half the normalized cross sections to twice of that. It is possible to adjust θ to focus the beam if we know the cross sections with accuracy 100% or perhaps even worse than that.

IV. Discussion

In principle, homogeneity of the gas density in the chamber is not necessary. All we need to know beside cross sections is the distribution of the gas density to adjust θ before injecting the beam into the reactor chamber. If the gas density is inhomogeneous but the distribution of the density is stationary, it is then no problem to set the right value for θ. If not stationary, the response time of the magnetic lens should be fast. It may be possible that the main current in the magnetic lens remains constant and the current for correction (~ 2%) is varied fast.

In the case of a rarefied background gas the density of electrons produced temporarily (e.g. pulse length of 10 ns) is much less

than that of the beam particles. However, such electrons are trapped in the deep electrostatic potential well of the beam. These accumulated electrons move with the beam. In this way, the current is also partially neutralized.

In the partially neutralized beam, there may be instabilities like wiggle modes and surface modes [9]. Both of them have essentially the same growth rate ω_b which is the beam plasma frequency as follows:

$$\omega_b = \left(\frac{n_b e^2 (1-f)}{m_i \varepsilon_o}\right)^{1/2} .$$

From $n_b = I/(e\beta c\pi R^2)$,

$$\omega_b = 4.0 \times 10^5 \frac{(1-f)^{1/2}}{R} ,$$

where $I = 1$ kA and $\beta = 0.3$.

The maximum number of e-foldings is

$$\int_o^{t_f} \omega_b dt \leq 4.0 \times 10^5 \int \frac{dt}{R}$$

$$= 4.0 \times 10^5 \frac{L}{R_o v} \ell n \frac{r_o}{r_f} = 0.8 ,$$

where $L = 10$ m, $R_o = 0.20$ m, $R_o = 0.003$ m and $v = 10^8$ m/s. Thus, these instability modes do not seem significant.

The multiple scattering effect has a significant influence on the emittance value if the pressure of the background gas is rather high. The coefficient of the multiple scattering term has a quadratic dependence on the atomic number Z_g of the background gas. The multiple scattering term may be then significant in the case of a high Z_g gas like lead in spite of the low pressure.

The change of the emittance is given as follows [10,2]:

$$\frac{\partial \varepsilon^2}{\partial z} = \frac{8\pi Z_g (Z_g+1) e^4 n_g Z_{eff}^2 \ell n(137/Z_g^{1/3})}{(4\pi\varepsilon_o)^2 m_b^2 v^4 \gamma^2} R^2 \quad .$$

If we assume $R = R_o - (R_o - R_f) z/L$, we then get approximately with $Z_g = 82$,

$$\delta\varepsilon^2 = 2.9 \times 10^{-34} \, n_g \, Z_{eff}^2 \quad .$$

If $n_g = 3.6 \times 10^{17} \, m^{-3}$ (10^{-5} torr) and $Z_{eff} = 5$,

$\delta\varepsilon = 5.0 \times 10^{-8}$ (m·rad). The change of the emittance due to the multiple scattering is then negligible (about 0.1% change) under the condition of the pressure of 10^{-5} torr of a background lead gas.

V. Conclusion

The existence of a rarefied lead gas has a great influence on beam focusing. The effect of the higher charge state of the uranium ions due to stripping by the gas dominates the neutralization effect due to the electrons produced so that the focal spot radius becomes larger than in the vacuum case, while the change is the opposite in the case of a 1 torr nitrogen background gas.

Nevertheless, it is possible to focus the beam within 3 mm at $z = 10$ m in the current range of about 1 kA. However, it should be noted that the accuracy of θ (envelope angle at the entrance port) has to be within 0.5%.

Acknowledgements

The author would like to thank Dr. I. Hofmann very much for encouragement throughout this work and for many valuable discussions. He is also indebted to Prof. A. Schlüter, who kindly provided the opportunity for this study.

References

[1] BUCHANAN, H.L., CHAMBERS, F.W., LEE, E.P., YU, S.S., BRIGGS, R.J., and ROSENBLUTH, M.N., UCRL-82586 (1979)

[2] YU, S.S., BUCHANAN, H.L., CHAMBERS, F.W., and LEE, E.P., in Proceedings of the Heavy Ion Fusion Workshop, Brookhaven National Laboratory, Upton (1974) p.55

[3] KULCINSKI, G.L., et al., Progress Report for Heavy Ion Beam Fusion Reactor Design, University of Wisconsin (1980), unpublished

[4] LAWSON, J.D., "The Physics of Charged-Particle Beams", Clarendon Press, Oxford (1977)

[5] GILLESPIE, G.H., CHENG, K.T., and KIM, Y.K., in Proceedings of the Heavy Ions Fusion Workshop, Argonne National Laboratory (1978), p.175

[6] KIM, Y.K., in ERDA Summer Study of Heavy Ions for Inertial Fusions, LBL-5543 (1976), p.59

[7] BEARDEN, J.A. and BURR, A.F., "Atomic Energy Levels", Oak Ridge, Tenn. (1965)

[8] JESSE, W.P. and SADAUKIS, J., Phys.Rev.102, 389 (1956); 107, 766 (1957)

[9] JORNA, S. and THOMPSON, W.B., in ERDA Summer Study of Heavy Ions for Inertial Fusions, LBL-5543 (1976), p.92

[10] LEE, E.P. and COOPER, R.K., Particle Accelerators 7, 83 (1976)

Figure Captions

Fig.1: Numerically calculated equipotential curves in a U^+ beam of cylindrical shape with uniform density distribution. In this case the length of the beam is 100 cm, the radius is 10 cm and I = 1 kA.

Fig.2a: The change of the envelope radius of the ion beam during propagation in vacuum (I = 1 kA; $\theta = -2.05 \times 10^{-2}$).

b: Under the same condition of a), except that a background gas of lead (10^{-5} torr) exists in the chamber. The curves of Z_{eff} and neutralization ratio f are also shown. The beam is only partially neutralized.

Fig.3a: Under the same condition of Fig.2b), except that $\theta = -2.13 \times 10^{-2}$.

b: The current is reduced to I = 800 A from the case a).

Fig.4a: Under the condition of $\theta = -2.12 \times 10^{-2}$ and I = 1 kA

b: I = 800 A

c: I = 900 A

Fig.5: The changes of the spot size R_s at the position z = 10 m, the focal spot radius R_f and the distance Δz of the focal point from z = 10 m as function of θ. The symbol $\Delta\theta$ (normalized to the case in Fig.3a) means $(-2.13\times10^{-2}-\theta)/2.13\times10^{-2}$.

Fig.6a: The change of the envelope radius during propagation in a background gas of lead with 2×10^{-5} torr and I = 1 kA, $\theta = -2.12 \times 10^{-2}$. Compare with Fig.4a).

b: The change of R_s, R_f and Δz varied as a function of the gas pressure p. The other conditions are the same as those of a).

Fig.7a: The change of the envelope radius during propagation in a background gas of nitrogen (the pressure is 1 torr). The curves of Z_{eff} and the ratio of the density of the

produced plasma to the beam density are also shown. Two different curves are calculated with two different models:
CLAS refers to the classical binary collision model and UPP to the upper limit cross sections with the Born approximation.
$\theta = -2.00 \times 10^{-2}$ and I = 1 kA.

b: The distribution of charge states of the ions in the beam at four different z distances from the entrance port. Under the same condition of a).

Fig.8: The changes of the spot size R_s at z = 10 m, the focal spot radius R_f and the distance Δz from the focal position to the position z = 10 m as a function of the cross sections used. The cross sections are normalized to the value resulting from the classical binary collision model. I = 1 kA, p = 10^{-5} torr (lead gas).

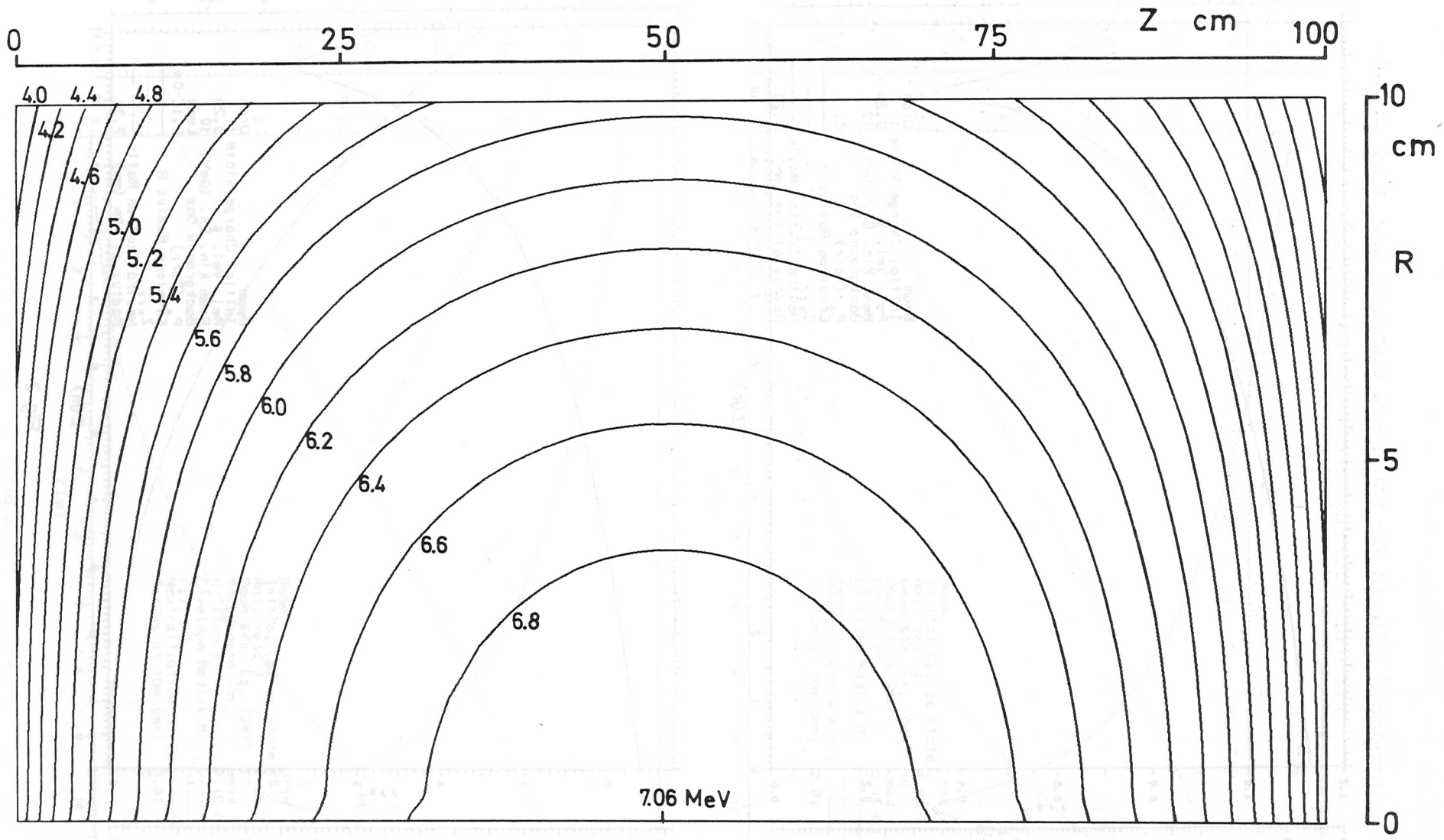
0
25
50
75
Z cm
100
4.0
4.2
4.4
4.6
4.8
5.0
5.2
5.4
5.6
5.8
6.0
6.2
6.4
6.6
6.8
7.06 MeV
10
cm
R
5
0

Fig. 1

a)

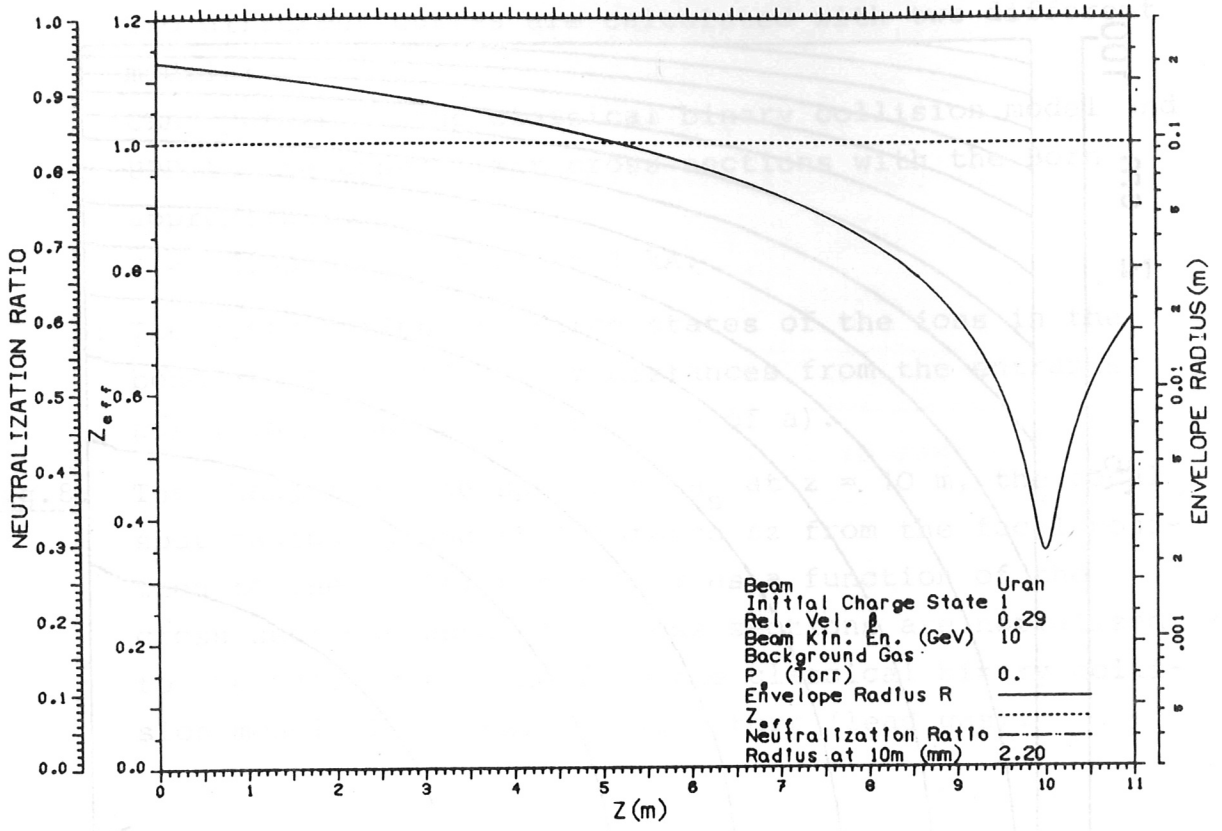
NEUTRALIZATION RATIO
Z_{eff}
ENVELOPE RADIUS (m)
Z (m)
Beam Uran
Initial Charge State 1
Rel. Vel. β 0.29
Beam Kin. En. (GeV) 10
Background Gas
P (Torr) 0.
Envelope Radius R
Z_{eff}
Neutralization Ratio
Radius at 10m (mm) 2.20

b)

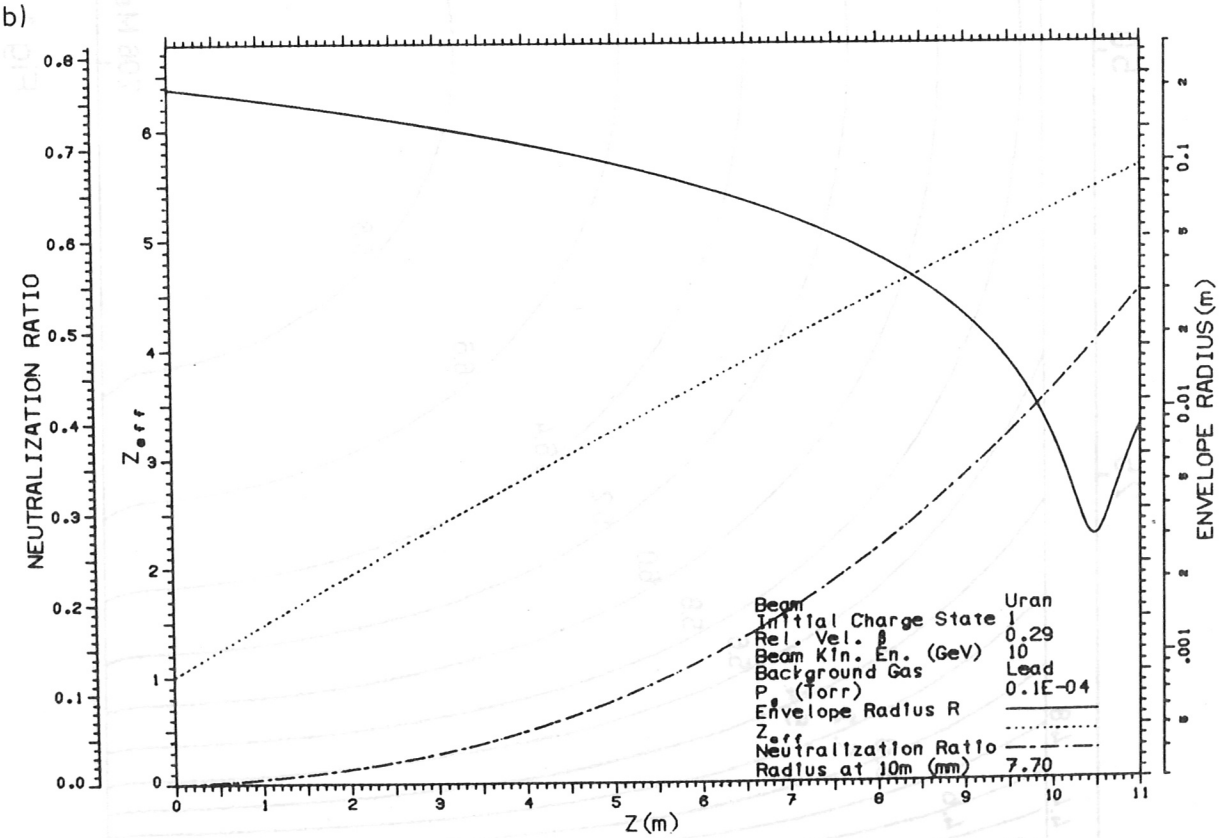
NEUTRALIZATION RATIO
Z_{eff}
ENVELOPE RADIUS (m)
Z (m)
Beam Uran
Initial Charge State 1
Rel. Vel. β 0.29
Beam Kin. En. (GeV) 10
Background Gas Lead
P (Torr) 0.1E-04
Envelope Radius R
Z_{eff}
Neutralization Ratio
Radius at 10m (mm) 7.70

Fig. 2

a)

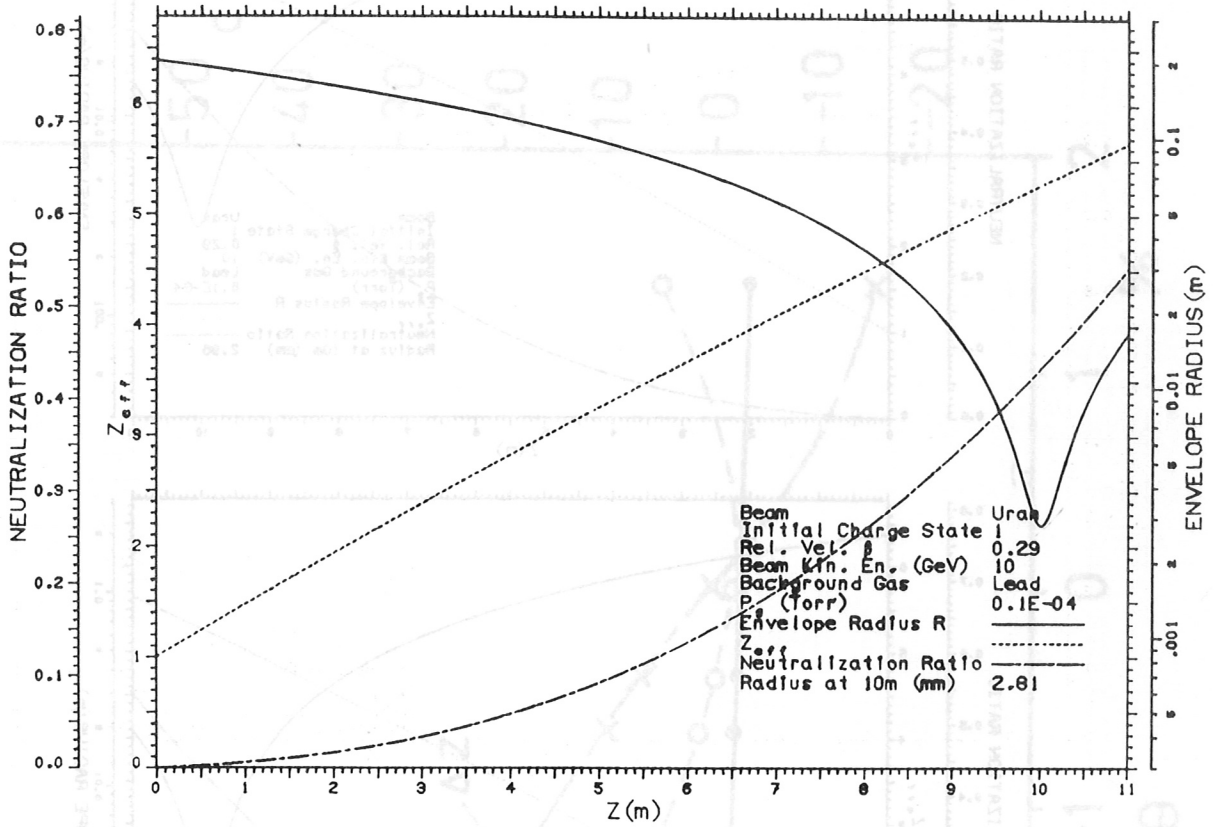
NEUTRALIZATION RATIO
Z_{eff}
Z (m)
ENVELOPE RADIUS (m)
Beam Uran
Initial Charge State 1
Rel. Vel. β 0.29
Beam Kin. En. (GeV) 10
Background Gas Lead
P_g (Torr) 0.1E-04
Envelope Radius R
Z_{eff}
Neutralization Ratio
Radius at 10m (mm) 2.81

b)

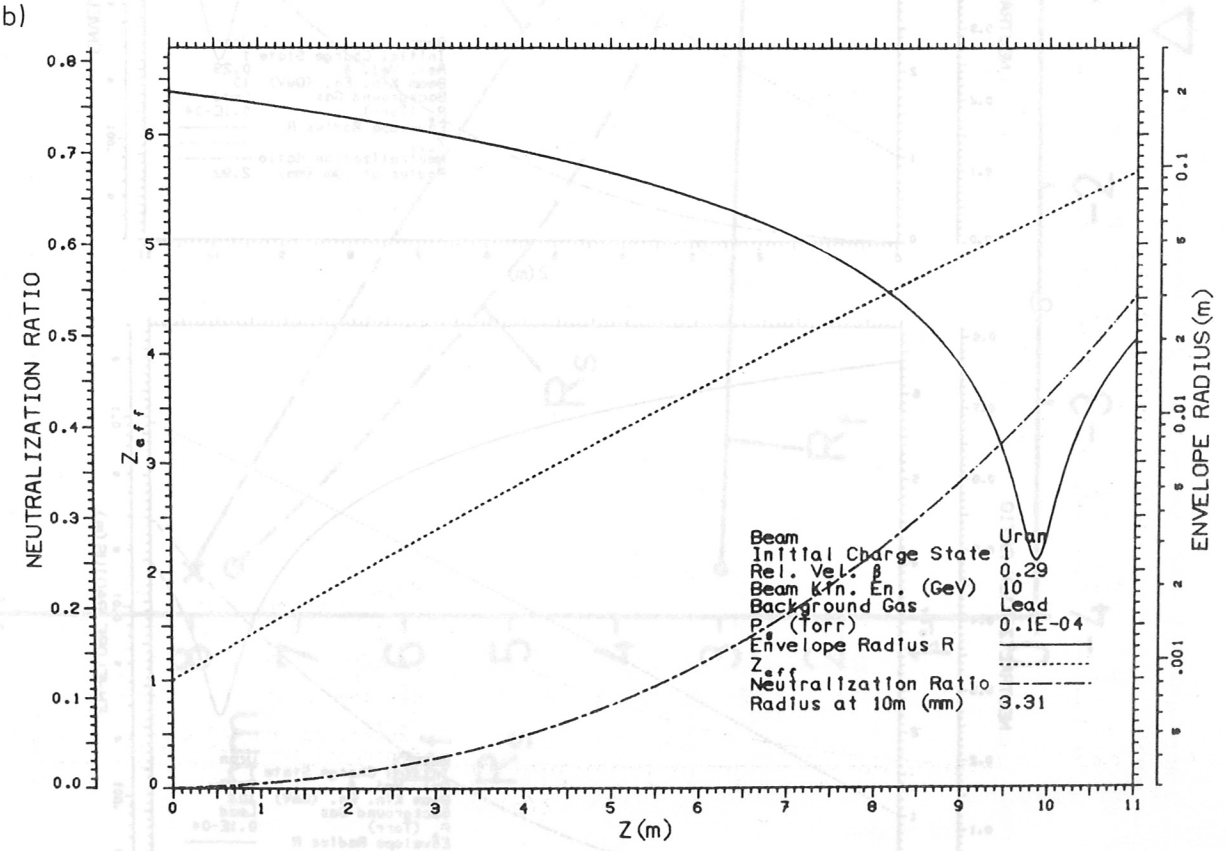
NEUTRALIZATION RATIO
Z_{eff}
Z (m)
ENVELOPE RADIUS (m)
Beam Uran
Initial Charge State 1
Rel. Vel. β 0.29
Beam Kin. En. (GeV) 10
Background Gas Lead
P_g (Torr) 0.1E-04
Envelope Radius R
Z_{eff}
Neutralization Ratio
Radius at 10m (mm) 3.31

Fig. 3

a)

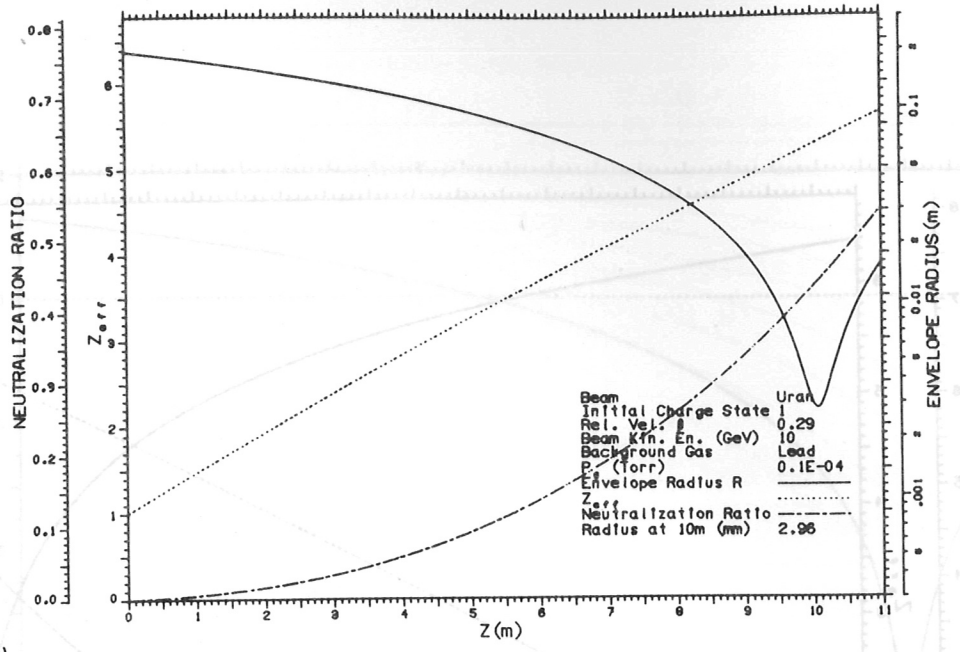
NEUTRALIZATION RATIO
ENVELOPE RADIUS (m)
Z (m)
Beam Uran
Initial Charge State 1
Rel. Vel. β 0.29
Beam Kin. En. (GeV) 10
Background Gas Lead
P (Torr) 0.1E-04
Envelope Radius R
Z_eff
Neutralization Ratio
Radius at 10m (mm) 2.96

b)

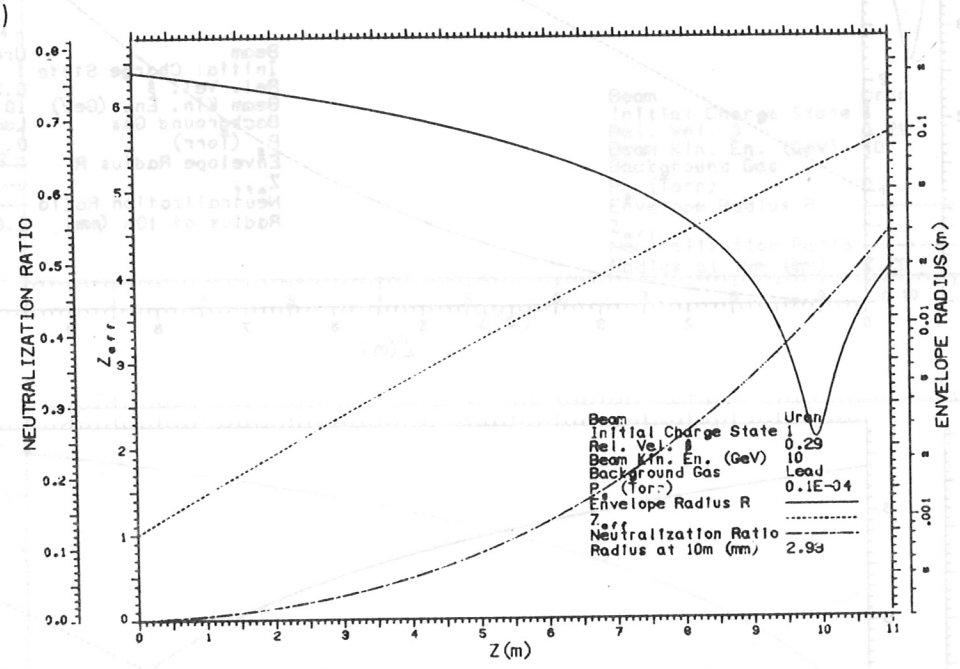
NEUTRALIZATION RATIO
ENVELOPE RADIUS (m)
Z (m)
Beam Uran
Initial Charge State 1
Rel. Vel. β 0.29
Beam Kin. En. (GeV) 10
Background Gas Lead
P (Torr) 0.1E-04
Envelope Radius R
Z_eff
Neutralization Ratio
Radius at 10m (mm) 2.93

c)

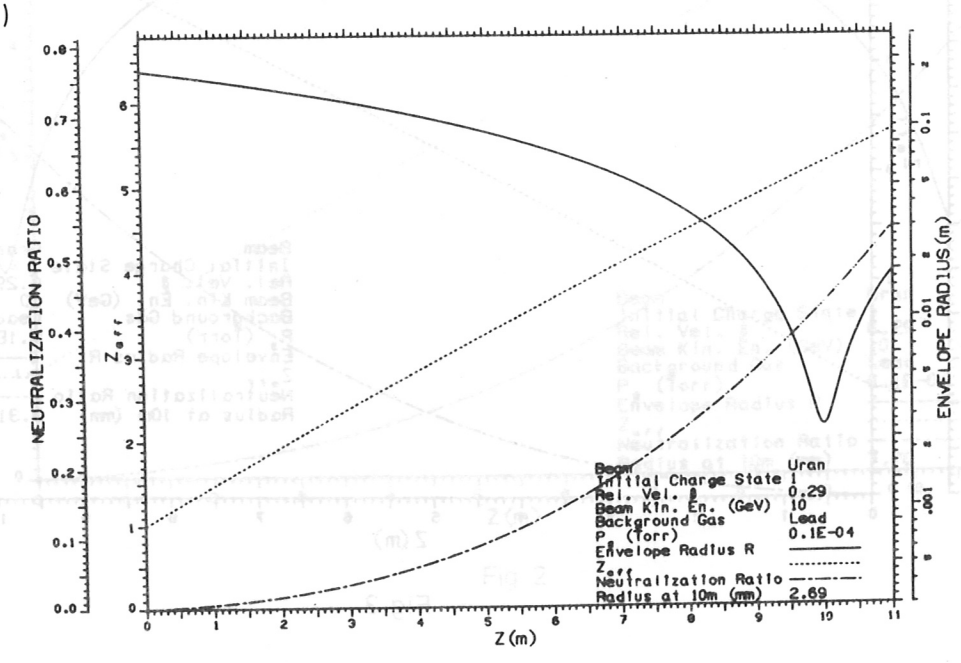
NEUTRALIZATION RATIO
ENVELOPE RADIUS (m)
Z (m)
Beam Uran
Initial Charge State 1
Rel. Vel. β 0.29
Beam Kin. En. (GeV) 10
Background Gas Lead
P (Torr) 0.1E-04
Envelope Radius R
Z_eff
Neutralization Ratio
Radius at 10m (mm) 2.69

Fig. 4

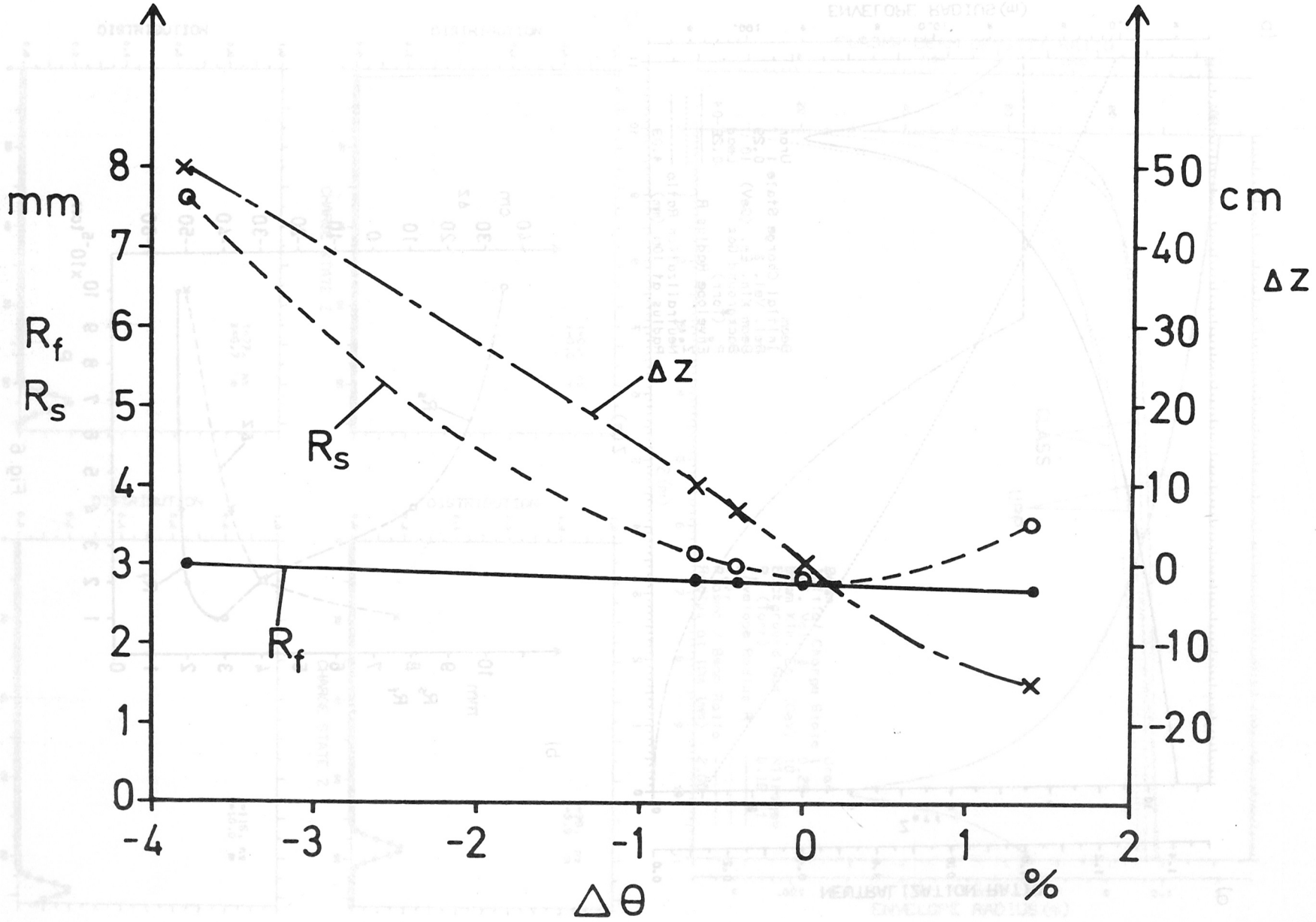
mm
R_f
R_s
8
7
6
5
4
3
2
1
0
R_s
ΔZ
R_f
-4
-3
-2
-1
0
1
2
$\Delta\theta$
%
50
40
30
20
10
0
-10
-20
cm
ΔZ

Fig. 5

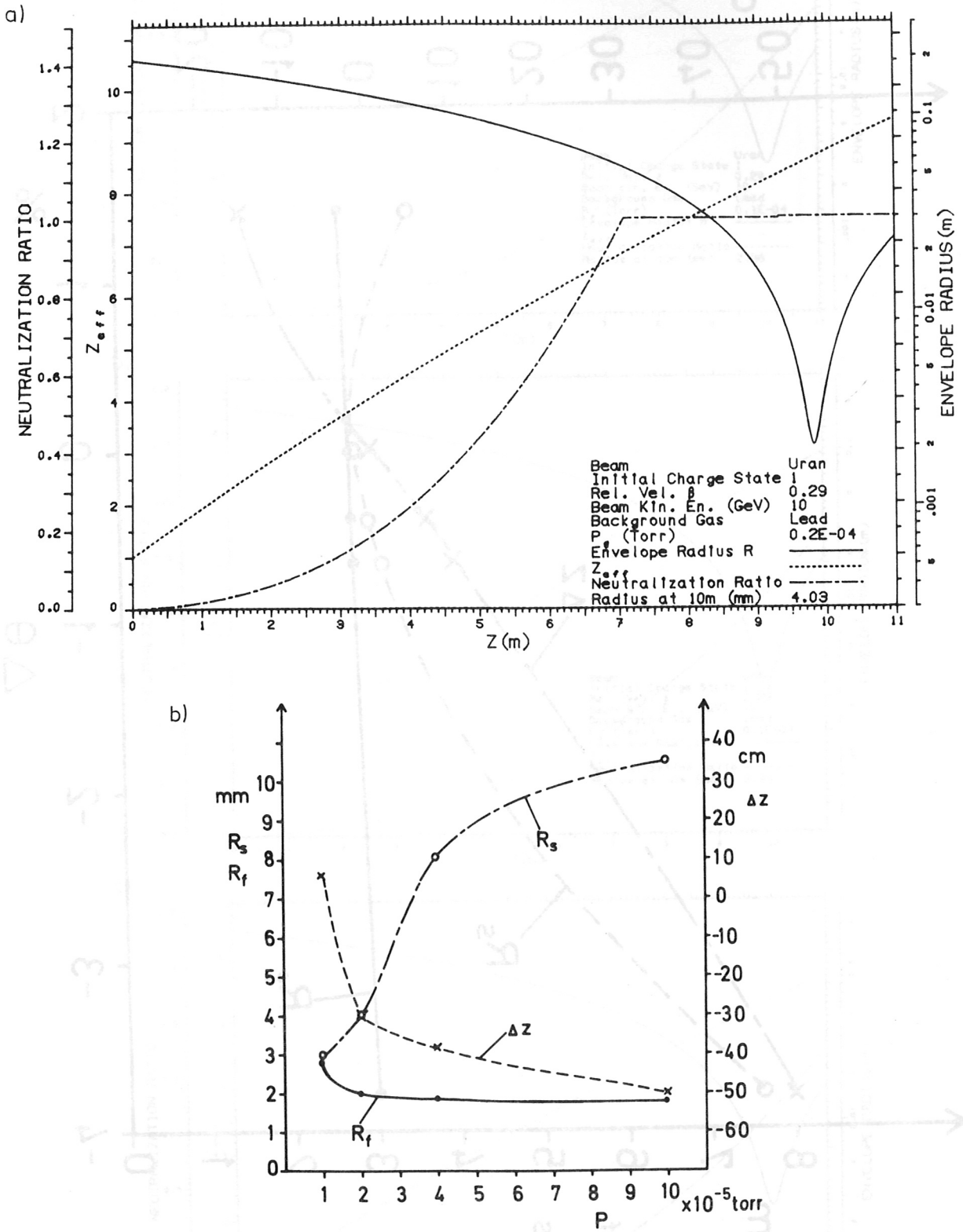
a)
NEUTRALIZATION RATIO
Z_{eff}
ENVELOPE RADIUS (m)
Z (m)
Beam Uran
Initial Charge State 1
Rel. Vel. β 0.29
Beam Kin. En. (GeV) 10
Background Gas Lead
P_g (Torr) 0.2E-04
Envelope Radius R
Z_{eff}
Neutralization Ratio
Radius at 10m (mm) 4.03
b)
mm
R_s
R_f
cm
ΔZ
R_s
ΔZ
R_f
P
$x10^{-5}$ torr

Fig. 6

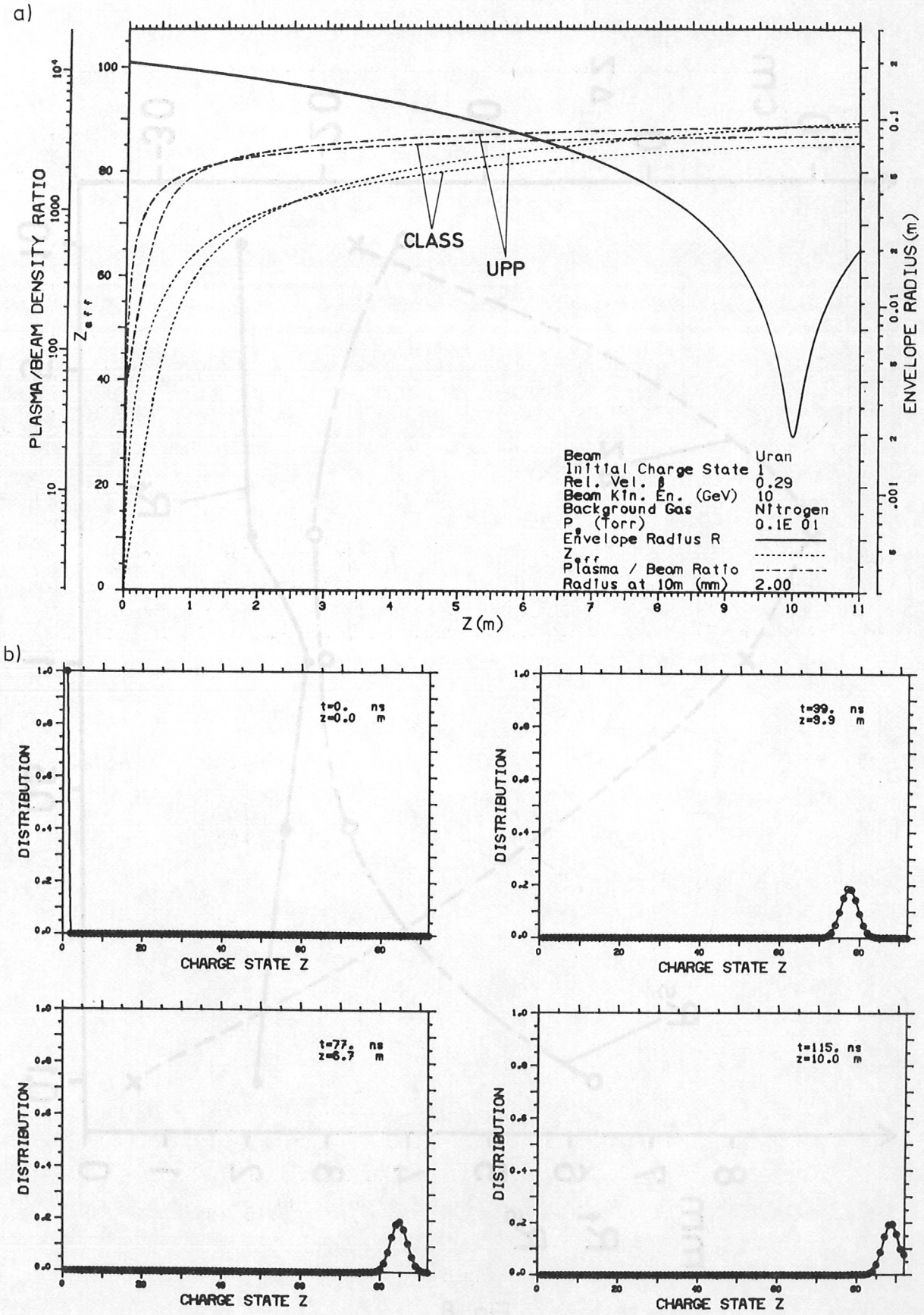
a)
PLASMA/BEAM DENSITY RATIO
ENVELOPE RADIUS (m)
Z (m)
Z_{eff}
CLASS
UPP
Beam Uran
Initial Charge State 1
Rel. Vel. β 0.29
Beam Kin. En. (GeV) 10
Background Gas Nitrogen
P_g (Torr) 0.1E 01
Envelope Radius R
Z_{eff}
Plasma / Beam Ratio
Radius at 10m (mm) 2.00
b)
DISTRIBUTION
CHARGE STATE Z
t=0. ns
z=0.0 m
t=39. ns
z=3.9 m
t=77. ns
z=6.7 m
t=115. ns
z=10.0 m

Fig. 7

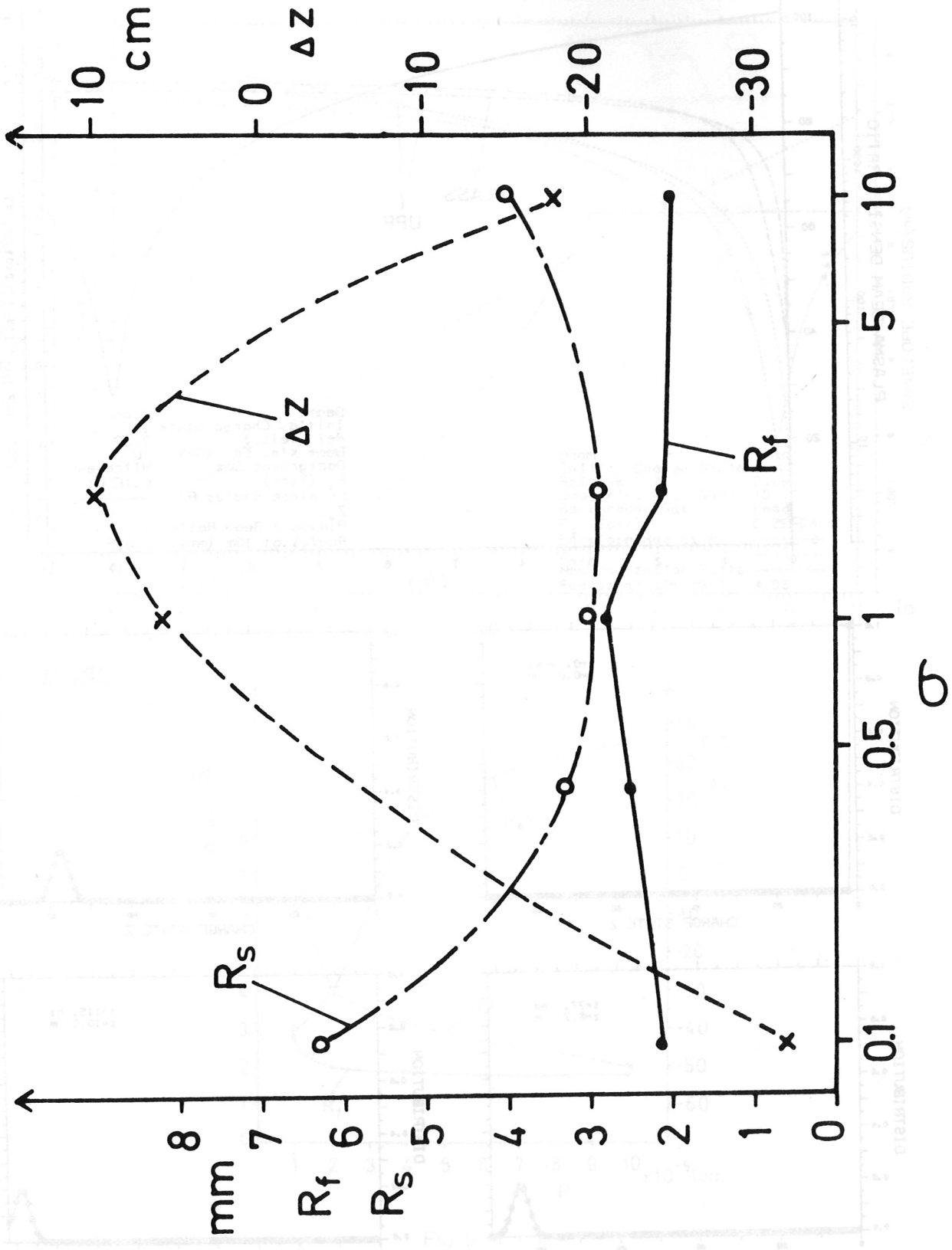

Fig. 8